

**DESIGN AND ANALYSIS OF PIEZOELECTRIC
CONFIGURATION FOR RAINDROP ENERGY
HARVESTER**

MUHAMMAD IZRIN BIN IZHAB

UNIVERSITI SAINS MALAYSIA

2018

**DESIGN AND ANALYSIS OF PIEZOELECTRIC CONFIGURATION FOR
RAINDROP ENERGY HARVESTER**

by

MUHAMMAD IZRIN BIN IZHAB

**Thesis submitted in fulfilment of the
requirements for the degree of
Master of Science**

November 2018

ACKNOWLEDGEMENT

First and above all, I praise God, the almighty for providing me this opportunity and granting me the capability to proceed successfully this research project. I would like to express my thanks to my supervisor, Dr Zuraini Binti Dahari for her guidance and support during my work on this project. Her patient guidance in monitoring my laboratory experiments and numerous information on enhancing my writing skills. Besides, I would like to thank Prof Madya Dr Asrulnizam Bin Abd Manaf, his ideas are much appreciated.

I would like to thank the lab technician, En Amir Bin Hamid for assisting using the laboratory equipment. I also would like to thank my friends for being great companions throughout completing this research project as well as their excellent support.

Finally, I would like to thank my loving parents and siblings for their valuable support, understanding and advice. This thesis would not have been possible without their support.

Last but not least, I would like to thank University Science Malaysia for providing research grant. This work was supported by Research University Grant, 1001/PELECT/814243 and Bridging Grant, 304/PELECT/6316125.

TABLE OF CONTENTS

	Page
ACKNOWLEDGEMENT	ii
TABLE OF CONTENTS	iii
LIST OF TABLES	vi
LIST OF FIGURES	viii
LIST OF ABBREVIATIONS	xiii
LIST OF SYMBOLS	xiv
ABSTRAK	xvii
ABSTRACT	xix
CHAPTER ONE: INTRODUCTION	
1.1 Background of Research	1
1.2 Problem Statement	3
1.3 Research Objectives	4
1.4 Research Scope and Limitation	5
1.5 Thesis Outline	6
CHAPTER TWO: LITERATURE REVIEW	
2.1 Introduction	7
2.2 Overview of Raindrop Characteristics	7
2.3 Raindrop Energy Harvesting via Piezoelectric	11
2.3.1 Operation Principle of Piezoelectric Raindrop Energy Harvester	11
2.3.2 Analytical Modelling of Piezoelectric Raindrop Energy Harvester Output	11
2.4 Ongoing Research on Piezoelectric Raindrop Energy Harvester	16
2.5 Basic Operation of AC-DC Power Converter	26
2.5.1 Half-Wave Rectifier	28
2.5.2 Full-wave Rectifier	30
2.5.3 Voltage Doubler	32
2.6 Ongoing Research on AC-DC Power Converter in PREH and PEH	33
2.7 Analysis of Ongoing Research on Raindrop Energy via Piezoelectric	37

2.8	Summary	42
-----	---------	----

CHAPTER THREE: METHODOLOGY

3.1	Introduction	43
3.2	Research Methodology	43
3.3	Experimental Setup	46
3.4	Investigation on Different PVDF Piezoelectric Configurations for PREH	50
3.4.1	Single PVDF Piezoelectric	52
3.4.2	X-Shaped PVDF Piezoelectric	54
3.4.3	Double Layer PVDF Piezoelectric	56
3.5	Development of AC-DC Power Converter Circuitry for PREH	57
3.5.1	Simulation for AC-DC Power Converter	61
3.5.2	Half-wave Rectifier	62
3.5.3	Full-wave Rectifier	63
3.5.4	Voltage Doubler	66
3.6	Development of Energy Storage Circuit for PREH	67
3.7	Summary	69

CHAPTER FOUR: RESULT AND DISCUSSION

4.1	Introduction	70
4.2	Preliminary Experimental Results	70
4.2.1	Analysis of PVDF Piezoelectric Thickness	71
4.2.2	Analysis of Various Heights of Water Droplet Impact	72
4.2.3	Analysis of Various Diameters of Water Droplet	73
4.3	Experiment of Different Configurations of PVDF Piezoelectric for PREH	75
4.3.1	Analysis of Peak to Peak Voltage and Frequency	75
4.3.2	Analysis of RMS Voltage and Current	82
4.3.3	Analysis of AC Output Power	85
4.4	Simulation Results of AC-DC Power Converter	89
4.4.1	Half-wave Rectifier	89
4.4.2	Full-wave Rectifier	91
4.4.3	Voltage Doubler	92

4.5	Experimental Results of AC-DC Power Converter Circuitry for PREH	92
4.5.1	Analysis of Half-wave and Full-wave Rectifier for PREH	93
4.5.2	Analysis of Different Values of Capacitor Filter for Full-wave Rectifier	101
4.5.3	Analysis of Different Values of Capacitor Filter for Voltage Doubler	106
4.6	Experimental Results of Energy Storage Circuit for PREH	110
4.7	Summary	112

CHAPTER FIVE: CONCLUSION AND RECOMMENDATION

5.1	Conclusion	113
5.2	Recommendation	114

REFERENCES	115
-------------------	------------

APPENDICES

Appendix A: Data collection and calculation

Appendix B: Datasheet

LIST OF PUBLICATIONS

LIST OF TABLES

	Page
Table 1.1: Top 10 country with highest average precipitation (Data.worldbank.org, 2016).	2
Table 2.1: Properties of precipitation (Perera <i>et al.</i> , 2014).	8
Table 2.2: Comparison of ongoing research on PREH system.	39
Table 2.3: Comparison of ongoing AC-DC power converter research.	41
Table 3.1: Experiment parameters for single PVDF piezoelectric.	54
Table 3.2: Parameter for X-Shaped PVDF piezoelectric experiment.	56
Table 3.3: Parameter for double layer PVDF piezoelectric experiment.	57
Table 3.4: Details of parameters for simulation process.	61
Table 3.5: Parameters for the half-wave rectifier experiments.	63
Table 3.6: Parameters for the full-wave rectifier experiments.	64
Table 3.7: Parameters for the voltage doubler experiments.	66
Table 4.1: Comparison of V_{P-P} and gradient of slope at different configurations of piezoelectric.	77
Table 4.2: Comparison of open-load voltage and frequency for different configurations.	80
Table 4.3: Comparison of voltage and phase difference between 1 st and 2 nd layer for different configurations.	81
Table 4.4: Summary the voltage and current improvement.	84
Table 4.5: Summary improvement of AC output power.	87
Table 4.6: Parameters performance for single PVDF piezoelectric.	87
Table 4.7: Parameters performance for X-Shaped PVDF piezoelectric.	88
Table 4.8: Parameters performance for double layer PVDF piezoelectric.	88
Table 4.9: Parameters for different types of diode.	93
Table 4.10: Frequency of half-wave and full-wave rectifier.	97

Table 4.11:	Rectifier efficiency of double layer PVDF piezoelectric.	100
Table 4.12:	Performance of full-wave rectifier with difference capacitances using multiple drops.	105
Table 4.13:	Performance of voltage doubler with different capacitances using multiple drops.	108
Table 4.14:	Summary of the performance full-wave rectifier and voltage doubler.	109

LIST OF FIGURES

	Page
Figure 2.1: Hamburger bun shaped of the raindrop (Fitzgibbons, 2013).	7
Figure 2.2: Mode ‘33’ and ‘31’ of piezoelectric device (Biswas <i>et al.</i> , 2009)	14
Figure 2.3: Propagation direction of piezoelectric device (a) mode ‘31’ and (b) mode ‘33’(Kim <i>et al.</i> , 2013).	15
Figure 2.4: Output voltage waveform of the piezoelectric in PREH.	15
Figure 2.5: PVDF Piezoelectric embedded by plexiglass (Guigon <i>et al.</i> , 2008b).	17
Figure 2.6: The detail of the experimental setup (Grinspan and Gnanamoorthy, 2010).	18
Figure 2.7: The experimental setup using cantilever configuration (Vatansever <i>et al.</i> , 2011).	19
Figure 2.8: Five layers PZT piezoelectric cantilever structure (Al Ahmad and Jabbour, 2012).	19
Figure 2.9: The experimental setup for (a) water droplet form and (b) flow form (Morrison and Decker, 2015).	20
Figure 2.10: The preliminary study of PREH (a) experimental setup, (b) result of cantilever and bridge configuration (Wong <i>et al.</i> , 2015a).	21
Figure 2.11: Schematic diagram of multi-harvester array (Ilyas and Swingler, 2017).	23
Figure 2.12: Hardware piezoelectric holder for multi-harvester array (Chee <i>et al.</i> , 2016)	24
Figure 2.13: The experimental setup of three different rain conditions (Wong <i>et al.</i> , 2016).	25
Figure 2.14: Block diagram of the renewable energy generation system	26
Figure 2.15: Block diagram of AC-DC power converter of the PREH applications.	27
Figure 2.16: The half-wave rectifier (a) schematic diagram (b) input voltage waveform and (c) output voltage waveform.	29

Figure 2.17: The full-wave rectifier (a) schematic diagram (b) input voltage waveform and (c) output voltage waveform.	30
Figure 2.18: The voltage doubler (a) schematic diagram (b) input voltage waveform and (c) output voltage waveform.	32
Figure 2.19: The output voltage of open-circuit using $0.60 \mu F$ (Wong and Dahari, 2017).	35
Figure 2.20: Output voltage of full-wave rectifier (Ilyas and Swingler, 2017)	36
Figure 2.21: Graphical compilation of ongoing research on PREH system.	37
Figure 2.22: Statistical compilation of ongoing research on AC-DC power converter.	40
Figure 3.1: Process flow required for PREH system.	44
Figure 3.2: Configurations setup of (a) single, (b) X-Shaped and (c) double layer PVDF piezoelectric.	45
Figure 3.3: Overall experimental setup for PREH system using PVDF piezoelectric.	47
Figure 3.4: NE 300 New Era Just Infusion Syringe pump.	48
Figure 3.5: Flow chart for preliminary experimental investigation (a) different thickness of PVDF piezoelectric, (b) different heights of water droplet impact, (c) different diameters of water droplet.	49
Figure 3.6: Experimental flow chart for different PVDF piezoelectric configurations.	50
Figure 3.7: The exponential voltage equation approach.	52
Figure 3.8: Piezoelectric holder setup for single PVDF piezoelectric.	53
Figure 3.9: Piezoelectric holder setup for X-Shaped PVDF piezoelectric.	54
Figure 3.10: Circuitry connection for (a) series and (b) parallel connection.	55
Figure 3.11: Piezoelectric holder setup for double layer PVDF piezoelectric.	56
Figure 3.12: Flow diagram for AC-DC power converter.	57
Figure 3.13: Flow chart for investigation of the best rectifier circuit.	59
Figure 3.14: Flow chart for analysis of the best AC-DC power converter.	60

Figure 3.15: Schematic diagram of the half-wave rectifier.	62
Figure 3.16: Schematic diagram of PVDF piezoelectric connected in (a) series and (b) parallel of the half-wave rectifier.	63
Figure 3.17: Schematic diagram of the full-wave rectifier.	64
Figure 3.18: Schematic diagram of PVDF piezoelectric connected in (a) series and (b) parallel of the full-wave rectifier.	65
Figure 3.19: Schematic diagram of the best rectifier with PVDF piezoelectric connected in (a) series and (b) parallel of the full-wave rectifier.	65
Figure 3.20: Schematic diagram of the voltage doubler.	66
Figure 3.21: Schematic diagram of the voltage doubler with PVDF piezoelectric connected in (a) series and (b) parallel of the full-wave rectifier.	67
Figure 3.22: Flow chart of energy storage for PREH.	67
Figure 3.23: Schematic diagram of PREH connected with battery.	68
Figure 4.1: Output voltage PVDF piezoelectric with different thickness.	71
Figure 4.2: Piezoelectric for (a) thin PVDF layer, (b) thick PVDF layer and compression effect for (c) thin PVDF layer, (d) thick PVDF layer.	72
Figure 4.3: Output voltage of PVDF piezoelectric, V_{p-p} at different (a) height, (b) velocity, and (c) kinetic energy of the water droplet.	73
Figure 4.4: Output voltage of PVDF piezoelectric, V_{p-p} at different (a) diameters, (b) masses, and (c) kinetic energy of the water droplet.	74
Figure 4.5: Output voltage PVDF piezoelectric, V_{p-p} at different configurations for (a) overall graph, and (b) gradient of curve.	76
Figure 4.6: Tension during impact for (a) Four end supports of X-Shaped and (b) two end supports of double layer PVDF piezoelectric.	78
Figure 4.7: Voltage waveform of X-Shaped for (a) first layer and (b) second layer.	78
Figure 4.8: Voltage waveform of double layer for (a) first layer and (b) second layer.	79

Figure 4.9:	Contact area between 1 st and 2 nd layer of PVDF piezoelectric (a) X-Shaped and (b) double layer.	81
Figure 4.10:	Effective output voltage and current with different configurations of PVDF piezoelectric.	83
Figure 4.11:	AC output power, P_{AC} with different configurations of PVDF piezoelectric.	85
Figure 4.12:	Simulation result of the waveform of half-wave rectifier.	90
Figure 4.13:	Simulation result of the waveform of full-wave rectifier.	91
Figure 4.14:	Simulation result of the waveform of voltage doubler.	92
Figure 4.15:	Output voltage rectifier for (a) half-wave and (b) full-wave rectifier using double layer PVDF piezoelectric in series connection.	93
Figure 4.16:	Voltage waveform of double layer PVDF piezoelectric in series connection.	94
Figure 4.17:	Output voltage rectifier for (a) half-wave and (b) full-wave rectifier using double layer PVDF piezoelectric in parallel connection.	95
Figure 4.18:	The duration of complete vibration of (a) half-wave and (b) full-wave rectifier.	95
Figure 4.19:	Duration of complete vibration of (a) half-wave and (b) full-wave in series connection and (c) half-wave and (d) full-wave in parallel connection.	96
Figure 4.20:	Voltage waveform of (a) PREH voltage, (b) half-wave rectifier and (c) full-wave rectifier.	98
Figure 4.21:	Average output voltage of (a) half-wave and (b) full-wave in series connection and (c) half-wave and (d) full-wave in parallel connection.	99
Figure 4.22:	V_{DC} of double layer PVDF piezoelectric in (a) series and (b) parallel connection interface with full-wave rectifier and capacitor filter.	102
Figure 4.23:	V_{DC} against X_C of double layer PVDF piezoelectric in (a) series and (b) parallel connection interface with full-wave rectifier and capacitor filter.	102

Figure 4.24: Output voltage capacitor filter for (a) single drop and (b) multiple drops.	103
Figure 4.25: Ripple voltage of full-wave rectifier using multiple drops for double layer PVDF piezoelectric in (a) series and (b) parallel connection.	104
Figure 4.26: Voltage discharged at (a) 22 nF and (b) 73 nF.	104
Figure 4.27: Ripple voltage at (a) 73 nF and (b) 150 nF.	105
Figure 4.28: V_{DC} of double layer PVDF piezoelectric in (a) series and (b) parallel connection interface with voltage doubler.	106
Figure 4.29: Ripple voltage of voltage doubler for double layer PVDF piezoelectric in (a) series and (b) parallel connection.	107
Figure 4.30: Ripple voltage of voltage doubler for double layer PVDF piezoelectric in series connection at (a) lowest capacitance and (b) highest capacitance.	107
Figure 4.31: Ripple voltage of voltage doubler for double layer PVDF piezoelectric in parallel connection at (a) lowest capacitance and (b) highest capacitance.	108
Figure 4.32: Output DC Voltage of (a) full-wave rectifier and (b) voltage doubler.	109
Figure 4.33: Output voltage of battery at (a) initial drop (b) final drop.	111

LIST OF ABBREVIATIONS

2S3P	Two series three parallel
AC	Alternating Current
AC-DC	Alternating Current to Direct Current
CWCVD	Cockcroft Walton Cascade Voltage Doubler
DC	Direct Current
DSD	Drop Size Distribution
HT	Heavy Thunderstorms
KFCVD	Karthus Fisher Cascade Voltage Doubler
LED	Light Emitting Diode
LSR	Light Stratiform Rain
MFC	Macro Fiber Composite
MSR	Moderate Stratiform Rain
NiMH	Nickel Metal Hydride
PEH	Piezoelectric energy harvester
PREH	Piezoelectric raindrop energy harvester
PVDF	Polyvinylidene Fluoride
PZT	Lead Zirconate Titanate
SSHI	Synchronised switch harvesting on inductor

LIST OF SYMBOLS

C	Capacitor
c_f	Drag coefficient
d	Piezoelectric strain constant
D	Diode
D_{drop}	Diameter of water droplet
D_n	Diameter of blunt needle
E	Electric field
f	Frequency
g	Gravitational constant
g_o	Piezoelectric voltage constant
h	Heights of water droplet
I	Precipitation intensity
I_{DC}	Average load current of the AC-DC power converter
I_{RMS}	Effective value of output current
I_s	Current supply
k	Ratio of the output electrical energy and the input mechanical energy
$K.E.$	Kinetic energy
m	Mass of raindrop
P	Polarisation generation
P_{AC}	AC power
P_{DC}	DC power
Q_M	Mechanical quality factor

R	Resistor
R_L	Resistive load
t	Time
v	Velocity
v_F	Fall velocity
V^+	Voltage at positive cycles
V^-	Voltage at negative cycles
V_o	Initial voltage
$V(t)$	Exponential voltage of piezoelectric
$V_{Piezoelectric}$	Voltage of piezoelectric
V_{AC}	AC voltage
V_{DC}	DC voltage
V_f	Forward voltage
V_P	Peak voltage
V_{P-P}	Peak to peak voltage
V_{PVDF}	PVDF piezoelectric generator
V_{Ripple}	Ripple voltage
V_{RMS}	Effective value of the output voltage
ω_0	Piezoelectric resonant frequency
$\Delta\omega$	Deviation in applied frequency
x	Induce strain magnitude
γ	Water surface stress
ρ_{water}	Density of water
ρ_{air}	Density of air

ε	Permittivity constant
ε_0	Permittivity piezoelectric
τ	Time constant
η	Efficiency

REKABENTUK DAN ANALISA PENUKAR KUASA UNTUK PENUAI TENAGA TITISAN HUJAN PIEZOELEKTRIK

ABSTRAK

Dekad yang lalu telah menyaksikan kemajuan yang pesat dalam tenaga boleh diperbaharui daripada sumber yang boleh diperbaharui seperti getaran mekanikal, suria, angin dan biomas. Berdasarkan tinjauan ilmiah, titisan hujan mempunyai potensi yang besar sebagai sumber tenaga yang boleh diperbaharui untuk sistem penuai tenaga titisan hujan piezoelektrik (PREH). Dalam kajian ini, sistem PREH dengan penukar kuasa AC-DC yang sesuai telah dibina. Objektif penyelidikan ini adalah untuk mencirikan dan membandingkan pelbagai konfigurasi piezoelektrik Polyvinylidene Fluoride (PVDF) serta menganalisis prestasi pelbagai jenis penukar kuasa AC-DC untuk sistem PREH. Peralatan pam picagari NE 300 digunakan untuk menghasilkan hujan tiruan dan diletakkan pada ketinggian 1.3 m di atas penjana piezoelektrik PVDF. Tiga konfigurasi piezoelektrik iaitu tunggal, bentuk-X dan dua lapisan dicirikan dan dibandingkan untuk menentukan prestasi terbaik berdasarkan kuasa yang dijana. Kemudian, konfigurasi terbaik piezoelektrik PVDF digunakan dalam penukar kuasa AC-DC. Litar berbeza penukar kuasa AC-DC seperti penerus gelombang separuh, penerus gelombang penuh dan penggandaan voltan telah dibandingkan untuk memilih penukar kuasa AC-DC yang sesuai untuk sistem PREH. Akhirnya, voltan keluaran penukar kuasa AC-DC telah digunakan dalam litar simpanan tenaga. Hasil dapatan menunjukkan bahawa piezoelektrik PVDF dua lapisan menghasilkan kuasa AC tertinggi iaitu (12.11 μ W) dengan peningkatan 196.09% daripada piezoelektrik PVDF

tunggal. Manakala piezoelektrik PVDF berbentuk X dan piezoelektrik PVDF tunggal menghasilkan $7.72 \mu\text{W}$ dan $4.09 \mu\text{W}$ masing-masing. Bagi litar penggandaan voltan didapati adalah penukar kuasa AC-DC yang berkesan dengan voltan DC tertinggi ialah 1.49 V diikuti oleh penerus gelombang penuh, 1.31 V . Akhir sekali, kajian ini juga mendapati bahawa PREH dari titisan berterusan pada 70 ml/min dengan 60 ml jumlah isi padu air dapat mengecas bateri dari 990 mV ke 995 mV dalam masa 2:26 minit.

DESIGN AND ANALYSIS OF POWER CONVERTER FOR PIEZOELECTRIC RAINDROP ENERGY HARVESTER

ABSTRACT

The past decade has been witnessed a huge growth in a renewable energy from renewable resources such as mechanical vibration, solar, wind and biomass. Based on literature review, raindrops have a huge potential as a renewable resource for a piezoelectric raindrop energy harvester (PREH) system. In this study, the PREH system with a suitable AC-DC power converter is developed. The objectives of this research are to characterise and compare different configurations of Polyvinylidene Fluoride (PVDF) piezoelectric as well as to analyse different types of AC-DC power converter performance for PREH system. NE 300 syringe pump equipment was used to produce artificial raindrops and was located at 1.3 *m* above the PVDF piezoelectric generator. Three different configurations of piezoelectric which are single, X-Shaped and double layer were characterised and compared to determine the best performance in the term of output power generated. Then, the best configuration of PVDF piezoelectric was utilised in the AC-DC power converter. Different circuits of AC-DC power converter which are half-wave rectifier, full-wave rectifier and voltage doubler were compared to choose the suitable AC-DC power converter for PREH system. Finally, the output voltage of the AC-DC power converter was utilised in the energy storage circuit. The results revealed that the double layer PVDF piezoelectric generated the highest AC output power (12.11 μW) with the 196.09% improvement from the single PVDF piezoelectric. Whereas, the X-Shaped PVDF piezoelectric and

the single PVDF piezoelectric generated 7.72 μW and 4.09 μW respectively. Furthermore, voltage doubler was found to be an effective AC-DC power converter with the highest DC voltage of 1.49 V followed by the full-wave rectifier, 1.31 V . Finally, this study also found that the PREH from multiple drops at 70 ml/min with 60 ml volume of water can charge the battery from 990 mV to 995 mV within 2:26 minutes.

CHAPTER ONE

INTRODUCTION

1.1 Background of Research

The miniature electronic device development with a low power has been offered an alternative approach in a scavenging energy (Mitcheson *et al.*, 2008). These devices have the potential to be powered from the energy harvested. The past decade has witnessed a huge growth in a renewable energy harvester from renewable sources such as mechanical vibrations (Dutoit *et al.*, 2005), solar (Raghunathan *et al.*, 2005), wind (Billinton and Bagen, 2006) and biomass (Paine *et al.*, 1996). These have led to a raindrop energy harvester development using piezoelectric materials. Such renewable solution has been considered a viable alternative to a rainy environment.

Piezoelectric raindrop energy harvester (PREH) is a unique type of renewable energy generation system which consists of kinetic energy of raindrop and piezoelectric generator. The PREH is utilised to convert the impact of raindrops into the electrical energy. The most common piezoelectric generator applied in the PREH system are Polyvinylidene Fluoride (PVDF) and Lead Zirconate Titanate (PZT).

The raindrops have a huge potential to perform as a renewable resource for the PREH system. According to precipitation data in Data.worldbank.org (2016), Malaysia is in the top 10 highest average precipitation per year with 2875 mm per year. Table 1.1 shows the average precipitation at different country.

Table 1.1: Top 10 country with highest average precipitation (Data.worldbank.org, 2016)

Country	Average Precipitation, <i>mm/year</i>
Colombia	3240
Sao Tome and Principe	3200
Papua New Guinea	3142
Solomon Islands	3028
Panama	2928
Costa Rice	2926
Malaysia	2875
Brunei Darussalam	2722
Indonesia	2702
Bangladesh	2666

According to Ortechnologies.net (2016), which accumulates the average precipitation per month in 40 weather station in our country, Malaysia has a high potential in implementing raindrop energy harvesting. The data of average precipitation per month in Malaysia is shown in Appendix A.

In addition, a few researches explored the average precipitation at various countries such as Malaysia, Indonesia, Philippines, Myanmar and India was over 2000 *mm* (Chua *et al.*, 2016; Costa and Foley, 1998). Syafrina *et al.* (2015) proposed a study on the trend of precipitation in Malaysia. In her study, the maximum average precipitation per hour for extreme rainfall seasons in Peninsular Malaysia were recorded (Syafrina *et al.*, 2015). The data rainfall seasons in Peninsular Malaysia is summarised in Appendix A.

However, harvesting energy from the impact of the raindrop generated an unstable and low voltage (Wong and Dahari, 2017). Hence, the implementation of a power converter is required to control the output voltage of the PREH. Over the past few years, there have been great attention and focus on power converter for various applications such as an electrical grid control system (Venkataramanan *et al.*, 1996),

energy harvester (Song *et al.*, 2003), an inverter system (Mazumdar *et al.*, 2002) and low-power on-chip (Ramadass and Chandrakasan, 2007).

Generally, low power application such as light-emitting diode (LED) (Suzuki *et al.*, 2008), a self-powered system (Peng *et al.*, 2014), and energy storage (Sodano *et al.*, 2005) required a constant DC voltage to operate the device. However, the output voltage generated from the PREH is in the form of damped AC voltage. Hence, implementing an AC-DC power converter is essential to convert the damped AC voltage into DC voltage. The AC-DC power converter comprises three basic circuits which are half-wave rectifier, full-wave rectifier and voltage doubler.

In this study, PREH system can be classified into four components which are an impact of a raindrop, piezoelectric generator, AC-DC power converter and load. The impact of the raindrop is focused on single and multiple drops. Next, the three different configurations of the piezoelectric generator are investigated to determine the satisfactory configuration in a term of power generated. Then, three basic circuits of an AC-DC power converter are analysed to decide the suitable circuit for PREH system. Finally, the output DC voltage is connected to the load which is energy storage to store the electrical energy.

1.2 Problem Statement

Prior research demonstrated that harvesting raindrop energy from piezoelectric materials has always been convincing potential for low power applications (Guigon *et al.*, 2008a). However, the generated output power from PREH system is in the micro-watt (μW) range and still unsatisfactory (Wong and Dahari, 2017). Hence, several techniques have been carried out to enhance the output power of the PREH system.

Over the past few years, X-Shaped and double layer piezoelectric configuration have been characterised and investigated to enhance the output power of the PREH system. However, the investigation on the X-Shaped piezoelectric only limited to the simulation process. Besides, multi-layer piezoelectric configuration that are implemented on PREH system only focused on double layer configuration as more layer will lead to piezoelectric rigidity and ineffective output voltage generated (Al Ahmad, 2014; Guigon *et al.*, 2008b). In addition, PREH system require AC-DC power converter to convert and control the AC voltage into DC voltage for low power applications. Energy storage using battery with several distinctive features of the battery are slow dissipation of charge, high efficiency of charging and discharging and durability in a term of long cycle life is utilised to store the harvested renewable energy (El-Sharkawi, 2004).

In this research, there are several addresses questions need to be resolved which are, the alternative ways to improve the generated output power of the piezoelectric generator from previous studies the types of AC-DC power converter that is suitable to be implemented in the present PREH system and the possibility to charge up the rechargeable battery.

1.3 Research Objectives

The main objectives of this research work are:

1. To characterise and compare different PVDF configurations of PVDF piezoelectric for PREH.
2. To analyse the performance of different types of AC-DC power converter for PREH.

1.4 Research Scope and Limitation

This research project focuses on the piezoelectric raindrop energy harvester (PREH) conversion from output AC voltage into DC voltage. There are three stages in this study which are, firstly to determine the highest output power generated from different PVDF piezoelectric configurations, to select the suitable AC-DC power converter for PREH system and finally, to develop the energy storage circuit.

In first stage, three configurations of PVDF piezoelectric were investigated to determine the highest output power. There are three configurations in this study which are single PVDF piezoelectric, X-Shaped PVDF piezoelectric and double layer PVDF piezoelectric. Besides, the dimension of PVDF piezoelectric was referred to the previous research (Wong and Dahari, 2017).

In the next stage, the three basic circuits which are half-wave rectifier, full-wave rectifier and voltage doubler is utilised to select the suitable circuit for AC-DC power converter. Initially, the three different types of diode were used in the AC-DC power converter to choose the suitable diode. Then, the half-wave and full-wave rectifier without capacitor filter is compared to verify the half-wave rectifier is ineffective for the energy harvester (Hart, 2011; Muhammad, 2014). Finally, the full-wave rectifier and voltage double with capacitor filter is compared to determine the best performance in term of suitable voltage level with low ripple voltage.

In the last stage, the generated output voltage from the suitable AC-DC power is connected to the rechargeable battery to justify the possibility of implementing the energy storage in the PREH system.

There are several limitations in this study. Firstly, the experiments are conducted in a laboratory by using artificial raindrop. Another limitation is the highest impact of a raindrop is restricted to the height from 1.3 *m* due to the limitation of the experimental setup.

1.5 Thesis Outline

This thesis comprises five chapters. Chapter One demonstrates the background of research, problem statements, research objectives, research scope and limitation of study. Chapter Two presents literature studies consists of the characteristics of a raindrop, raindrop energy via piezoelectric and AC-DC power converter for piezoelectric energy harvester (PEH) and piezoelectric raindrop energy harvester (PREH). Chapter Three discusses the research methodology and the experimental setup in this work. The methodology comprises preliminary investigation, investigation on different PVDF piezoelectric configuration, development of AC-DC power converter and development of energy storage circuit. Chapter Four demonstrates the result of preliminary investigation, experiments of different PVDF piezoelectric configuration, simulation and experiments of AC-DC power converter. Finally, Chapter Five presents the conclusion the overall research study and suggest some recommendation for future works.

CHAPTER TWO

LITERATURE REVIEW

2.1 Introduction

In this chapter, the characteristics of raindrop, the raindrop energy harvesting via piezoelectric and AC-DC power converter for piezoelectric energy harvester (PEH) and piezoelectric raindrop energy harvester (PREH) is presented. Previous works on the types of materials and configurations of the piezoelectric are reviewed to evaluate the efficiency of the piezoelectric generator of PREH system. Moreover, the ideal power converter for raindrop energy harvester methods is also discussed to determine the suitable AC-DC power converter.

2.2 Overview of Raindrop Characteristics

A shape of a raindrop is flattened on its lower surface and rounded curvature and also known as “hamburger bun shaped” (Fitzgibbons, 2013). The shape of the raindrop is illustrated as shown in Figure 2.1.

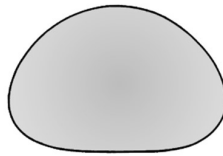


Figure 2.1: Hamburger bun shaped of the raindrop (Fitzgibbons, 2013).

Other than that, some researchers suggested the shape of the tiny raindrop is almost spherical (Beard *et al.*, 2010). As the size of the raindrop is increased, the shape of raindrop becomes flattened and the drag coefficient, c_f of the raindrop is increased.

The drag coefficient, which also known as the aerodynamics of the raindrop will affects the velocity of the raindrop (Boyd *et al.*, 2001). In other words, the size of the raindrop will influence the velocity of the raindrop.

Another researcher described the characteristics of the raindrop behaviour as unpredictable and complex (Lam *et al.*, 2012). The precipitation intensity, I and the drop size distribution (DSD) are the most common and widely used to characterise the parameters of the raindrop. Precipitation intensity is defined as the amount of precipitation water over a time (mm/hr) (Di Leo *et al.*, 2013; Torres *et al.*, 1994). Besides, the drop size distribution is defined as the total amount of raindrop count in specific raindrop diameter class (Das *et al.*, 2017; Marshall and Palmer, 1948).

Based on meteorology in the United States, there are four types of precipitations which are light stratiform rain (LSR), moderate stratiform rain (MSR), heavy thunderstorms (HT), and violent (Horstmeyer, 2011). Each type of precipitations has a specific size of the raindrop and precipitation intensity. Table 2.1 presents the four types of precipitation with precipitation intensity and the diameter of the raindrop.

Table 2.1: Properties of precipitation (Perera *et al.*, 2014)

Type of precipitation	Precipitation Intensity, mm/hr	Diameter of Raindrop, mm
Light Stratiform rain (LSR)	2 – 4	2.0
Moderate Stratiform rain (MSR)	5 – 9	2.6
Heavy Thunderstorms (HT)	10 – 40	5.0
Violent	> 50	> 5.0

From Table 2.1, the diameter of the raindrop is in the range between 2.0 mm to 5.0 mm while the violent type is greater than 5.0 mm . The diameter of the raindrop is increased as the precipitation intensity is increased (Perera *et al.*, 2014).

In 2009, Saikia *et al.* investigated and compared the raindrop size distribution (RSD) in India (Saikia *et al.*, 2009). They discovered the diameter of the raindrop during light stratiform rain was in the range between 0.1 mm to 2.8 mm. The pre-monsoon rainfall in the year 1993 and 2006 were compared and found the diameter of the raindrop is in the range between 0.2 mm to 4.5 mm.

Another study about DSD was also proposed by Marzuki *et al.* (2013) The four regions which are Kototabang, Pontianak, Manado and Biak in Indonesia were explored. The results showed the diameter of the raindrop was ranging from 0.4 mm to 8.5 mm (Marzuki *et al.*, 2013).

In 2014, Wong *et al.* predicted the diameter of the artificial raindrop using a syringe pump for PREH study (Wong *et al.*, 2014). The prediction involved photography and image processing to compare their results with the theoretical studied by (Guigon *et al.*, 2008b). Their results showed the photography and image processing method agreed with the theoretical result. The theoretical equation of the diameter of the raindrop is given by:

$$D_{drop} = \sqrt[3]{\frac{6 D_n \gamma}{\rho g}} \quad 2.1$$

Where D_{drop} is the diameter of water droplet, D_n is the external diameter of the needle, g is the gravitational constant (9.81 ms^{-2}), γ is water surface stress, and ρ is the density of water (1000 kgm^{-3}) (Guigon *et al.*, 2008a; Guigon *et al.*, 2008b).

Based on Chua *et al.* (2016), a mass of the raindrop can be calculated from the diameter of the raindrop using (Chua *et al.*, 2016):

$$m = \rho_{water} \frac{4}{3} \pi \left(\frac{D_{drop}}{2} \right)^3 \quad 2.2$$

Where ρ_{water} (1000 kgm^{-3}) is the density of the water, and D_{drop} is the diameter of the raindrop (Foote and Du Toit, 1969).

Another important parameter in the raindrop behaviour is the velocity of the raindrop (Helseth and Wen, 2017). Terminal velocity is used as a reference for the velocity of the raindrop due to various heights of the raindrop fall (Niu *et al.*, 2010). Terminal velocity is defined as the highest velocity attained by the raindrop. In the real situation, the raindrop will travel at constant maximum velocity due to air resistance (Kavanagh and Goldblatt, 2015). The velocity of the artificial raindrop can be determined using Equation (2.3) and Equation (2.4) (Range and Feuillebois, 1998).

$$v_F = \sqrt{\frac{g}{Z} (1 - e^{-2Zh})} \quad 2.3$$

$$Z = \frac{3c_f \rho_{air}}{8D_{drop} \rho_{water}} \quad 2.4$$

Where g is gravitational acceleration (9.81 ms^{-2}), c_f is the drag coefficient, ρ_{air} (1.225 kgm^{-3}) is the density of air, D_{drop} is diameter of droplet, and ρ_{water} is the density of water.

Other than that, the kinetic energy of the raindrop is defined as the energy from the vibration motion of piezoelectric (Halliday *et al.*, 2014). The kinetic energy, $K.E.$ can be calculated using Equation (2.5) (Wong *et al.*, 2014).

$$K.E. = \frac{1}{2} m v^2 \quad 2.5$$

Where m is the mass of the raindrop, and v is the velocity of the raindrop (Muhammad, 2014).

2.3 Raindrop Energy Harvesting via Piezoelectric

In this section, the characteristics of the piezoelectric is studied to understand the concept of an energy conversion between a kinetic energy and an electrical energy. Some applications of the piezoelectric in different researches are presented. In addition, the common piezoelectric material used in PREH is also demonstrated. The basic operation of the piezoelectric is explained. Finally, the detail analytical modelling of the generated output voltage in PREH is characterised.

2.3.1 Operation Principle of Piezoelectric Raindrop Energy Harvester

Piezoelectricity is an ability of certain materials to generate an electrical charge when force or vibration is subjected to the piezoelectric devices (Uchino, 2003). A characteristic of piezoelectricity is reversible. The electricity is generated when force or vibration is introduced. It also can produce the vibration when an electric field is applied. The piezoelectric device is chosen as an energy conversion between kinetic energy and electrical energy because it offers a reliable response when the piezoelectric device is subjected to the low impact of the raindrop (Grinspan and Gnanamoorthy, 2010).

Piezoelectricity is widely used in the devices for various applications such as biomedical applications (Zhou *et al.*, 2014), underwater instruments (Stansfield and Elliott, 2017) and energy harvester devices (Spies *et al.*, 2015). In Micro-Electro-Mechanical systems (MEMS) application, several types of piezoelectric materials are commonly used for example PVDF, PZT, Trifluoroethylene (TrFE), Barium Titanate (BaTiO_3) and Graphene Oxide (PMMA/GO) are commonly used.

The selection material of the piezoelectric is critical for the performance of PREH system. Generally, three prominent piezoelectric materials have been extensively used in PREH system which is PVDF, PZT and PMMA/Go (Chua *et al.*, 2016; Wong *et al.*, 2015a). PMMA/Go material was difficult to implement in the PREH systems due to low output power generated (Valentini *et al.*, 2013).

The PVDF piezoelectric was preferred in PREH compared to PZT piezoelectric. The advantage of PVDF piezoelectric is flexible, smoothness, tightness and environmental friendly properties. Besides that, PVDF piezoelectric generates an excellent performance of voltage and noiseless when a low impact force is applied (Grinspan and Gnanamoorthy, 2010). Other than that, the drawback of PZT piezoelectric material is rigid surface and brittle (Warude *et al.*, 2015).

There are several parameters equation that are extensively used in piezoelectric such as induced strain magnitude, induced electric field, voltage constant of piezoelectric, polarisation generation, electromechanical coupling factor, mechanical quality factor and voltage generated across the electrode plate (Uchino, 2009):

The induced strain magnitude, x is defined as the product of the strain constant of the piezoelectric, d and induced electric field, E . The expression of the x is given by:

$$x = dE \tag{2.6}$$

Subsequently, the induced electric field, E is defined as the multiplication of the voltage constant of the piezoelectric, g_o and external stress, X . The expression of the E is given by:

$$E = g_o X \tag{2.7}$$

Then, the voltage constant of the piezoelectric can be expressed by:

$$g_o = \frac{d}{\varepsilon_0 \varepsilon} \quad 2.8$$

Other than that, the polarisation generation, P is defined as the products of the strain constant of the piezoelectric, d and the external stress, X is given by:

$$P = dX \quad 2.9$$

Where d is strain constant, X is external stress, ε_0 is the permittivity constant and ε is the relative permittivity of the piezoelectric.

Besides, the electromechanical coupling factor, k is the ratio of the output electrical energy and the input mechanical energy as shown in Equation (2.10):

$$k^2 = \frac{\text{Stored electrical energy}}{\text{Input mechanical energy}} \quad 2.10$$

Apart from that, the expression of the mechanical quality factor of the piezoelectric, Q_M is given as:

$$Q_M = \frac{\omega_0}{2\Delta\omega} \quad 2.11$$

Where ω_0 is resonant frequency of the piezoelectric, and $\Delta\omega$ is deviation in applied frequency. The parameter of the mechanical quality factor of the piezoelectric is utilised to describe the electromechanical resonant spectrum sharpness. In addition, the voltage of piezoelectric, V can be expressed as:

$$V = \frac{Qx}{\varepsilon_0 \varepsilon A} \quad 2.12$$

Where Q is charge, x is displacement, ϵ_0 is electrical permittivity in a vacuum, ϵ is relative permittivity of piezoelectric material, and A is cross section area of electrode plate. deviation in applied frequency.

Generally, there are two coupling methods in the piezoelectric device which are mode '33' and '31'. Figure 2.2 illustrates the two coupling methods of piezoelectric device (Clark and Mo, 2009; Ramsay and Clark, 2001).

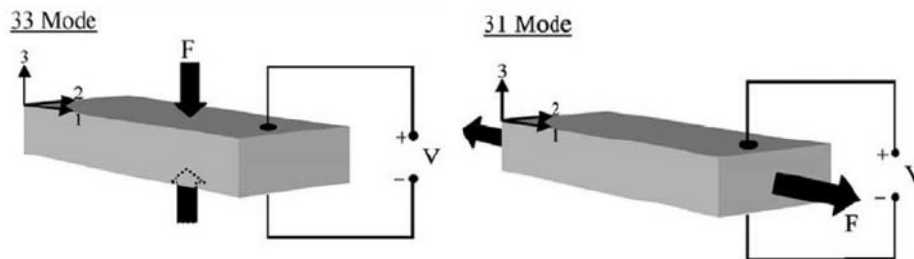


Figure 2.2: Mode '33' and '31' of piezoelectric device (Biswas *et al.*, 2009).

In mode '33' of the piezoelectric device, the mechanical force is applied in parallel to the poling direction. While in mode '31', the mechanical force is applied in perpendicular to the poling direction. In PREH systems, the mode '31' is recommended due to its efficiency in piezoelectric energy harvesting (PEH) applications (Baker *et al.*, 2005).

The propagation direction of piezoelectric for mode '33' and '31' was illustrated as shown in Figure 2.3. However, in PREH system mode '33' is needed as the direction of impact raindrop is vertical direction. Therefore, mode '33' is desired to utilise in the PREH system as the coupling method of piezoelectric in the PREH system is vertical direction.

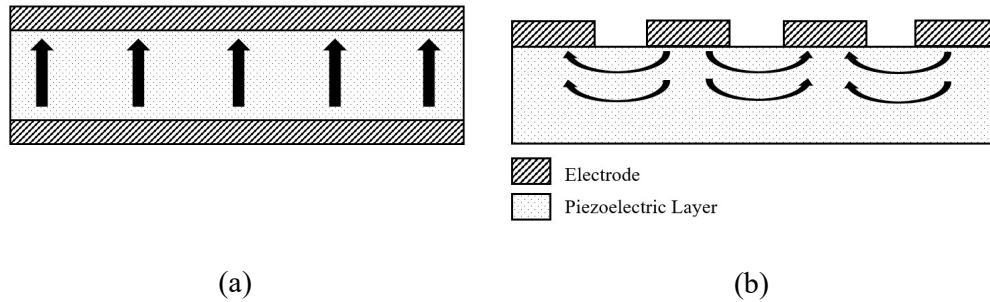


Figure 2.3: Propagation direction of piezoelectric device (a) mode '31' and (b) mode '33'(Kim *et al.*, 2013).

2.3.2 Analytical Modelling of Piezoelectric Raindrop Energy Harvester

Output

The purpose of this characterisation was to determine the piezoelectric generator performance and to demonstrate the analytical modelling output voltage of the piezoelectric (Ilyas and Swingler, 2015; Wong and Dahari, 2017; Wong *et al.*, 2015b). Figure 2.4 presents the general output voltage waveform of the PREH.

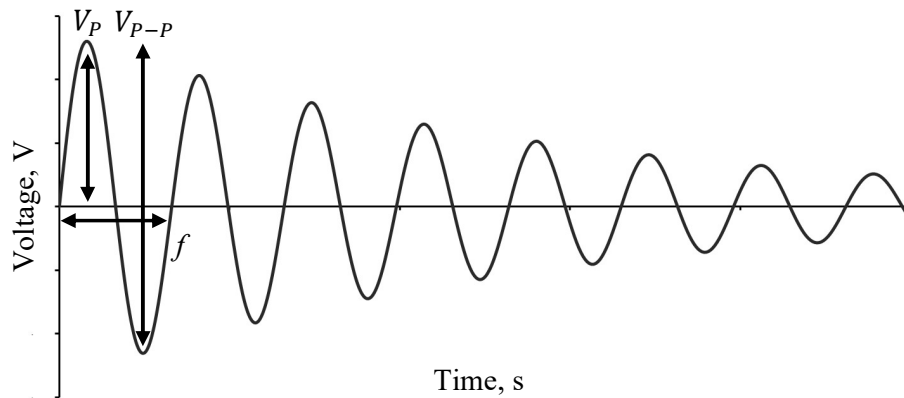


Figure 2.4: Output voltage waveform of the piezoelectric in PREH.

The performance of piezoelectric are evaluated using the following parameters (Ilyas and Swingler, 2015; Wong *et al.*, 2015b):

- The peak voltage of piezoelectric, V_p
- The peak to peak voltage of piezoelectric, V_{p-p}
- The frequency of piezoelectric, f

The expressions for the voltage, $V_{Piezoelectric}$ and exponential voltage, $V(t)$ equation of the piezoelectric are given as follows:

$$V_{Piezoelectric} = V(t) \sin (2\pi f) \quad 2.13$$

and

$$V(t) = V_o e^{-\frac{t}{\tau}} \quad 2.14$$

Where V_o is initial voltage, t is elapsed time and τ is time constant of the discharging voltage.

On the other hand, the effective value of the output voltage piezoelectric, V_{RMS} (Muhammad, 2014) is

$$V_{RMS} = \sqrt{\frac{1}{T} \int_0^T [V_{PVDF}]^2 dt}$$

$$V_{RMS} = \sqrt{\frac{1}{T} \int_0^T \left[V_o e^{-\frac{t}{\tau}} \sin (2\pi f) \right]^2 dt} \quad 2.15$$

The effective value of output current of piezoelectric, I_{RMS}

$$I_{RMS} = \frac{V_{RMS}}{R} \quad 2.16$$

To calculate the AC power of piezoelectric, P_{AC} the effective output voltage and current of piezoelectric are multiplied (Hart, 2011; Muhammad, 2014) to give:

$$P_{AC} = V_{RMS} I_{RMS} \quad 2.17$$

2.4 Ongoing Research on Piezoelectric Raindrop Energy Harvester

The earliest research on PREH was proposed by Guigon *et al.* (2008) using PVDF piezoelectric. The PVDF piezoelectric was chosen due to its flexibility, smoothness, tightness and environmentally friendly properties. Besides, the PVDF

piezoelectric was setup in a bridge configuration where both ends of PVDF piezoelectric were embedded by plexiglass (Guigon *et al.*, 2008b). Figure 2.5 shows the hardware PVDF piezoelectric holder.

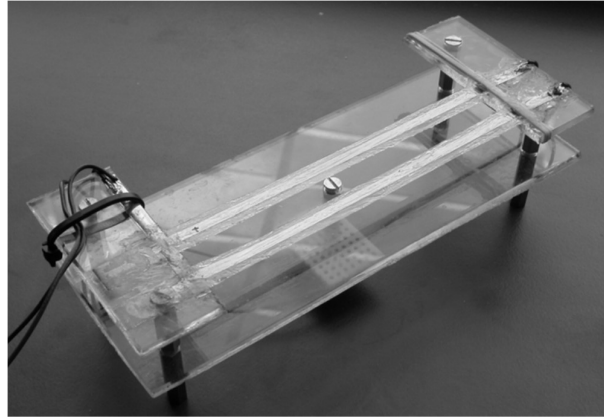


Figure 2.5: PVDF Piezoelectric embedded by plexiglass (Guigon *et al.*, 2008b)

They conducted three experiments to investigate the effects of the output voltage on the thickness of the PVDF piezoelectric and the diameter of the water droplet. The last experiment was to evaluate the PREH under artificial raindrop. The results showed the $25\ \mu\text{m}$ thick generated a higher voltage, ($V_p \approx 3\ \text{V}$) than $9\ \mu\text{m}$ ($V_p \approx 0.5\ \text{V}$). Besides, the $3\ \text{mm}$ diameter of the water droplet produced a higher voltage, ($V_p = 17.2\ \text{V}$) than that of $1.6\ \text{mm}$ ($V_p = 4.68\ \text{V}$). In addition, under the artificial raindrop with $2\ \text{m}$ height the generated voltage was $17.2\ \text{V}$ (Guigon *et al.*, 2008b).

In 2010, Grinspan and Gnanamoorthy studied the output voltage on various masses of the liquid droplet. In their experiment, they used three different liquid droplets which are water, hydraulic oil and lubricant oil (Grinspan and Gnanamoorthy, 2010). Then, the PVDF piezoelectric was used to measure the output voltage. Noted that they attached the PVDF piezoelectric to the solid surface. The author also emphasised that the PVDF piezoelectric was used due to its ability to produce high voltage signal with low noise at low impact force. Hence, the amplification process is

inessential. Figure 2.6 presents the experimental setup for various masses of the liquid droplet.

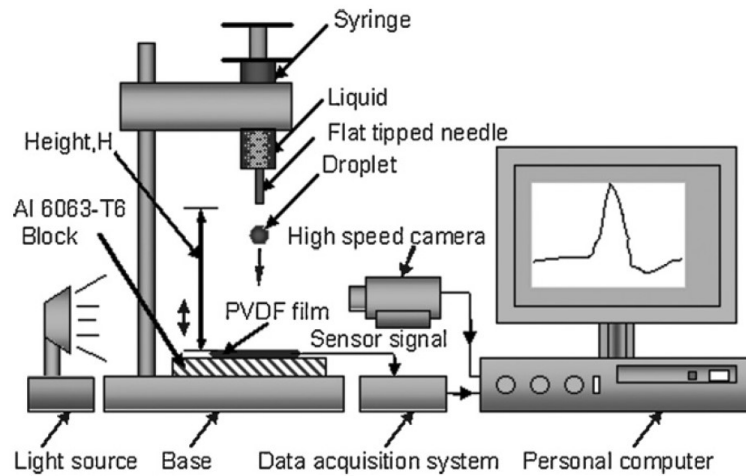


Figure 2.6: The detail of the experimental setup (Grinspan and Gnanamoorthy, 2010)

The results concluded the greatest weight of the liquid droplet generated the highest voltage. Other than that, the voltage increased as the velocity of the liquid droplet increased. Noted that the height of impact was adjusted to vary the velocity of the liquid droplet. Furthermore, at the same velocity (2.96 ms^{-1}) the water droplet generated the highest voltage (92.94 mV) (Grinspan and Gnanamoorthy, 2010).

In 2011, Vatansever *et al.* compared different materials and dimensions of the piezoelectric for raindrop experiment. The author conducted three experiments to analyse the effect of different material piezoelectric, the masses and the height of the water droplet. They also highlighted the PVDF advantages such as its lightweight, flexibility and low cost. The experiments were carried out using a cantilever configuration where the piezoelectric was fixed at one end. Figure 2.7 represents the experimental setup to compare different materials of piezoelectric.

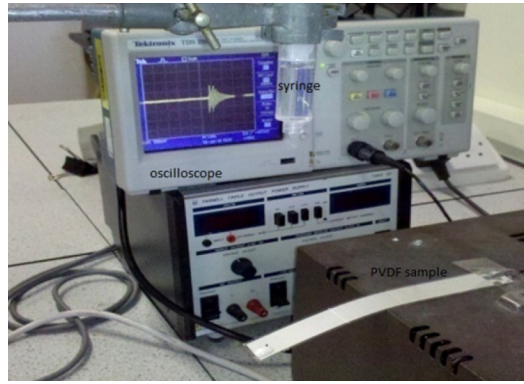


Figure 2.7: The experimental setup using cantilever configuration (Vatansever *et al.*, 2011)

Investigation of the piezoelectric materials revealed that PVDF piezoelectric generated higher voltage than Lead Zirconate Titanate, PZT piezoelectric. Apart from that, the greatest weight ($m = 50 \text{ mg}$) and the highest height ($h = 100 \text{ cm}$) of the water droplet generated the highest voltage ($V_p \approx 12 \text{ V}$) (Vatansever *et al.*, 2011).

From 2012 to 2014, Al Ahmad *et al.* discovered the multi-layer PZT piezoelectric in the cantilever configuration for piezoelectric water drop energy. The multi-layer PZT piezoelectric was fabricated using screen printing techniques. Then, the output voltage of each PZT piezoelectric was connected in a parallel connection. The author believed the multi-layer PZT piezoelectric can enhance the output power. Figure 2.8 presents the multi-layer PZT piezoelectric configuration.

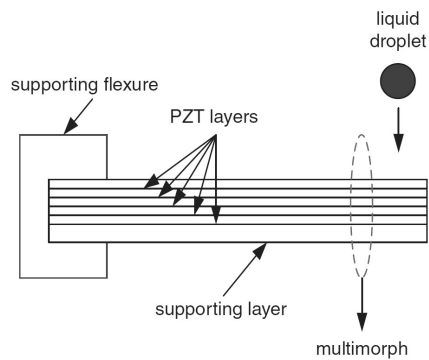


Figure 2.8: Five layers PZT piezoelectric cantilever structure (Al Ahmad and Jabbour, 2012)

Al Ahmad *et al.* performed three experiments in their study. The experiments were carried out to investigate the output voltage from three consecutive drops and multiple drops of the water droplet. The last experiment was to investigate the effect of different sizes of the water droplet on the output PZT voltage. Based on the results, multiple drops of the water droplet could generated up to 1 V. Furthermore, it was found that the output voltage increased as the size of the water droplet increased (Al Ahmad, 2014; Al Ahmad and Jabbour, 2012; Alkhaddeim *et al.*, 2012).

In 2015, Morrison and Decker compared the output voltage of the water droplet and flow form. In their study, they used the PVDF piezoelectric because it produced a high voltage ($\bar{V} = 2.38 \mu V$). The PVDF was attached to plexiglass (solid surface configuration) and the impacts drops were set at 5 cm height. Figure 2.9 presents the experimental setup in Morrison and Decker studied.

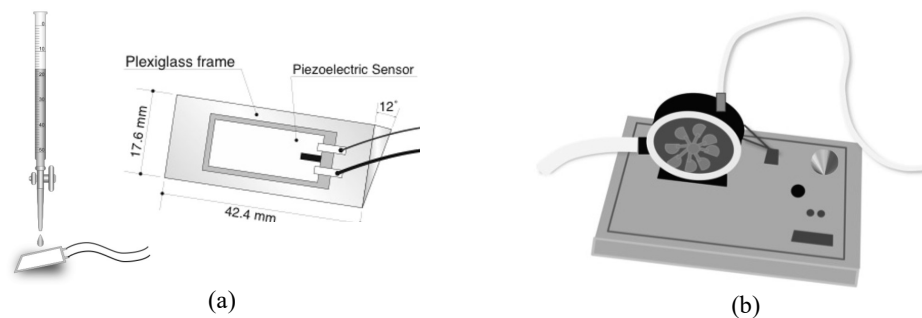


Figure 2.9: The experimental setup for (a) water droplet form and (b) flow form (Morrison and Decker, 2015)

Based on the results, the output voltage from both forms are almost similar. The water droplet form produced slightly higher voltage than flow form due to the inconsistency flow rate generated by hydroelectric turbine. The water droplet form generated $2.38 \mu V$ per 0.2 ml (Morrison and Decker, 2015).

In between 2014 to 2017, Wong *et al.* from the Universiti Sains Malaysia (USM) have conducted research on the raindrop energy via piezoelectric. At the earlier

stage, he performed a preliminary study on piezoelectric configuration. Figure 2.10 demonstrates the preliminary study on piezoelectric configuration.

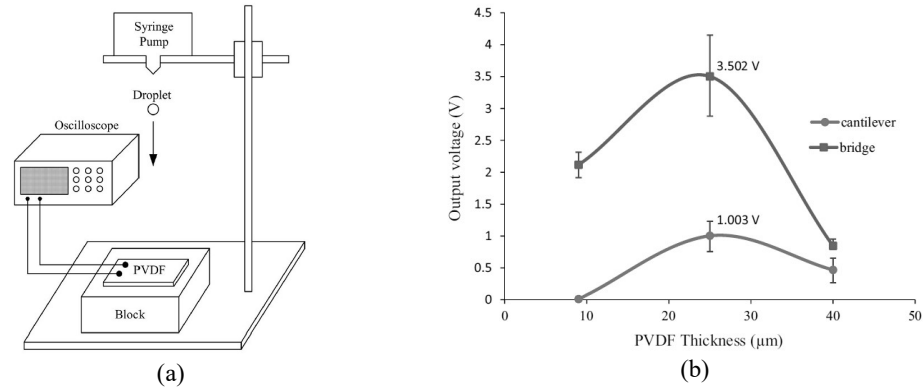


Figure 2.10: The preliminary study of PREH (a) experimental setup, (b) result of cantilever and bridge configuration (Wong *et al.*, 2015a).

From the results, the author concluded the bridge configuration generated higher voltage than cantilever configuration of PVDF piezoelectric. The bridge configuration generated 3.502 V which are three times higher than cantilever configuration of PVDF piezoelectric 1.003 V (Wong *et al.*, 2015a).

On further research, he extended his study on X-Shaped PVDF piezoelectric with different number of spokes (number of fixed ends). He designed the X-Shaped PVDF piezoelectric using two bridge PVDF piezoelectric. The investigation was carried out using the Finite Element Method (FEM) to discover the effect of the number of spokes PVDF piezoelectric on the output voltage generated. The result revealed the X-Shaped with four spokes generated higher voltage, 6.04 V than six spokes 3.92 V (Wong *et al.*, 2017a).

He also investigated the effect of different sizes and heights of the water droplet. The results proved that the bridge configuration generated higher voltage than cantilever configuration (4.22 V and 0.41 V respectively). In addition, he found that

the biggest diameter, (5.6 mm) and the highest height, (0.5 m) of the water droplet generated the highest voltage (4.22 V) (Wong and Dahari, 2017).

During 2015 to 2017, Ilyas and Swingler have studied the raindrop energy via piezoelectric. There are two studies in his research focused on PVDF piezoelectric (FS-2513P) with cantilever configuration (Ilyas and Swingler, 2015; Ilyas and Swingler, 2017).

At the initial stage, Ilyas and Swingler (2015) have proposed a technique to harvest energy from the impact of the raindrop. They applied two approaches in their study. The first approach is to investigate the output voltage of PVDF piezoelectric with various impact heights and resistive load. Meanwhile, the second approach is to model a multi-harvester array with different sizes of the area.

Based on their findings, the voltage increased as the impact height and resistance increased. Other than that, the output voltage generated by PVDF piezoelectric with cantilever configuration is 3.75 V. The modelled results revealed the output power increased as the area of the multi-harvester array was increased (Ilyas and Swingler, 2015).

In their recent study, Ilyas and Swingler (2017) implemented their previous modelling concept to perform the multi-harvester array. They carried out two experiments to study the output voltage from different surface condition using single piezoelectric and output performance of the multi-harvester array. Figure 2.11 illustrates the circuitry connection of multi-harvester array.

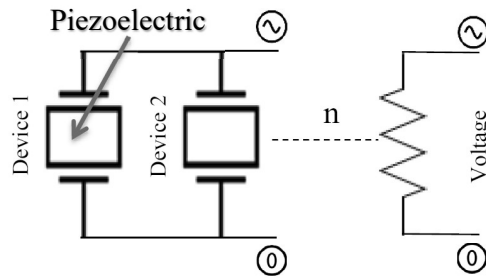


Figure 2.11: Schematic diagram of multi-harvester array (Ilyas and Swingler, 2017)

According to Ilyas and Swingler (2017), there are four different surfaces named dry and wet surface, Cellulose transparent tape material and the Vinyl Insulation tape material. The results revealed that there were no obvious differences in the output voltage of the PVDF piezoelectric using different surfaces. Apart from that, Ilyas and Swingler incorporated multi-harvester array using several PVDF piezoelectric connected in parallel connection. In their works, the impact of water droplets only hit one of PVDF piezoelectric and the other PVDF piezoelectric remain statics. Implementing multi-harvester array, the output voltage decreased as the number of PVDF piezoelectric increased. The results reported that the highest output voltage generated was 3.1 V (Ilyas and Swingler, 2017).

Meanwhile, Chee *et al.* (2016) proposed a study of a multi-harvester array using the synchronous drop timing of the single water droplet. They used the multi-harvester array in the bridge configuration to investigate different PVDF piezoelectric connections circuitry behaviour. Figure 2.12 presents the PVDF piezoelectric in the multi-harvester array configuration.

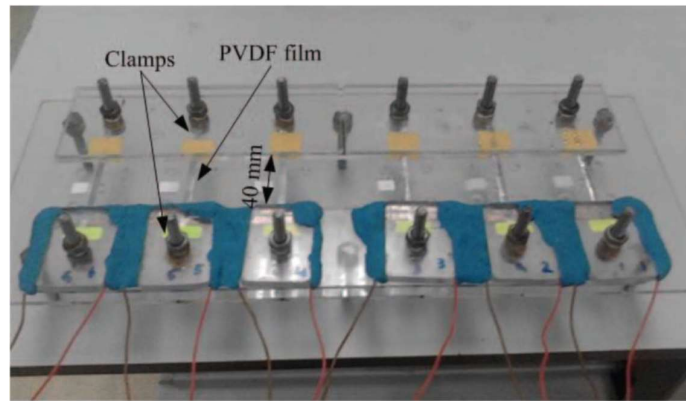


Figure 2.12: Hardware piezoelectric holder for multi-harvester array (Chee *et al.*, 2016)

The effect of different connection includes the series, parallel and combination of series and parallel connection on the output voltage were evaluated. The results concluded that the output voltage increased as the number of PVDF piezoelectric increased. In addition, the author highlighted the asynchronous drop timing will influence the output voltage generated. Chee *et al.* claimed the highest voltage generated is 1.87 V using the series and parallel combination connection (Chee *et al.*, 2016).

The researcher from the University of Nottingham have explored the total energy generated in three different rain conditions using PZT piezoelectric with cantilever configuration (Wong *et al.*, 2016). The spray-type rain simulator with different nozzles was used to investigate the output voltage of light, moderate and heavy rain in five minutes. The author also highlighted the problem using spray-type rain simulator is the velocity of the raindrop higher than terminal velocity and contradict with the theoretical calculation. The experimental setup of three different rain conditions using a spray-type rain simulator as shown in Figure 2.13.